Journal of Molecular Catalysis A: Chemical 355 (2012) 102–112

Contents lists available at SciVerse ScienceDirect

Journal of Molecular Catalysis A: Chemical

journal homepage: www.elsevier.com/locate/molcata

# Role of bifunctional catalyst 2-pyridone in the aminolysis of *p*-nitrophenyl acetate with *n*-butylamine: A computational study

Xiao-Qiang Liu [a], Lu Jin [a], Chan Kyung Kim [b], Ying Xue [a,*]

[a] College of Chemistry, Key Laboratory of Green Chemistry and Technology in Ministry of Education, Sichuan University, Chengdu 610064, PR China
[b] Department of Chemistry, Inha University, Incheon 402-751, Republic of Korea

ARTICLE INFO

*Article history:*
Received 6 October 2011
Accepted 1 December 2011
Available online 10 December 2011

*Keywords:*
Bifunctional catalyst
2-Pyridone and 2-hydroxypyridine
*p*-Nitrophenyl acetate
Aminolysis of ester
Zwitterionic intermediate

ABSTRACT

The possible catalytic effects of 2-pyridone and its tautomeric form 2-hydroxypyridine on the aminolysis reaction of *p*-nitrophenyl acetate with *n*-butylamine have been theoretically studied at the B3LYP/6-31+G(d,p) level of theory. Solvent effect of chloroform is assessed using the MP2/CPCM/6-31++G(d,p)//B3LYP/6-31+G(d,p) method. In our work, three possible mechanisms are considered for the title reaction. The first mechanism is concerted via a four-membered ring transition state assisted by supramolecular effect of the catalyst. The second mechanism undergoes two sequential steps, where the intermolecular proton transfer bridged by the catalyst is the rate-determining process. And the third mechanism, forming a zwitterionic intermediate, is also stepwise via three steps, nucleophilic addition, double-proton transfer, and elimination of leaving group. Our calculations give a detailed picture of the whole stepwise pathway through zwitterionic intermediates for the first time, and indicate that this mechanism is the most favored pathway both in the gas phase and in chloroform.



## 1. Introduction

In that aminolysis of ester is a primary process in the formation of peptide bond, there were numerous kinetic as well as mechanistic studies on these reactions in chemistry and biochemistry. The purposes of both experimental [1–14] and theoretical [15–26] studies were mainly to establish the effects of substrate such as ester structures and amine nature, medium, and catalysts on the reaction rate and mechanism. As shown in Scheme 1, three possible mechanisms were raised for the uncatalyzed reaction. Path A is concerted via a four-membered transition state, while paths B and C are stepwise via a neutral intermediate and a zwitterionic intermediate $T^{\pm}$, respectively. Zipse et al. theoretically investigated some model systems for the aminolysis of ester using *ab initio* methods and found that the reaction rate largely depended on the leaving group but little effect of acyl substituents [19]. In addition, the high priority for concerted pathway over the neutral stepwise pathway was established when esters with good leaving groups. Ilieva et al. [23] studied the aminolysis of methylformate with QCISD/6-31G(d,p) and B3LYP/6-31G(d) methods and found that the neutral stepwise and the concerted pathways have very similar activation energy, and the presence of aprotic solvent acetonitrile fully lowers all energy barriers. Jin et al. [26] found that the reaction prefers the concerted pathway to the neutral stepwise process in the gas phase and solutions concerning the aminolysis of phenylformate. From experimental observations, Menger et al. assumed that the breakdown of zwitterionic intermediate $T^{\pm}$ to products should be rate-determining in aprotic solvents [12,13]. Kinetics studies by Jencks and co-workers supported the intermediacy of $T^{\pm}$ in the general base catalysis aminolysis of alkyl esters [14].

Some researchers made efforts to theoretically study the stepwise pathway through zwitterionic intermediates [15,18,21,22]. Chalmet et al. [21] reported a theoretical study on the model reaction of ammonia and formic acid with the continuum model and did not predict a stable zwitterionic intermediate, whereas a local energy minimum was found by explicit consideration of four solvent water molecules. For the reaction of methylformate with ammonia, Ilieva et al. did not succeed in applying MP2/6-31G(d,p) method to identify zwitterionic transition states and intermediates [23]. They reported that two explicit water molecules are needed to obtain a very shallow minimum. Singleton and Merrigan [27] reported a resolution of the apparently conflicting mechanistic observations in ester aminolyses through modeling the isotope effects in zwitterion tetrahedral intermediates between methylformate and ammonia or hydrazine in water. They used the B3LYP/6-31G(d,p) method to calculate various solvated structures involving from four to eleven explicit water molecules; however, they failed to find global minima for these structures. Recently,

* Corresponding author. Tel.: +86 28 85418330.
*E-mail address:* yxue@scu.edu.cn (Y. Xue).

1381-1169/$ – see front matter © 2011 Elsevier B.V. All rights reserved.
doi:10.1016/j.molcata.2011.12.003

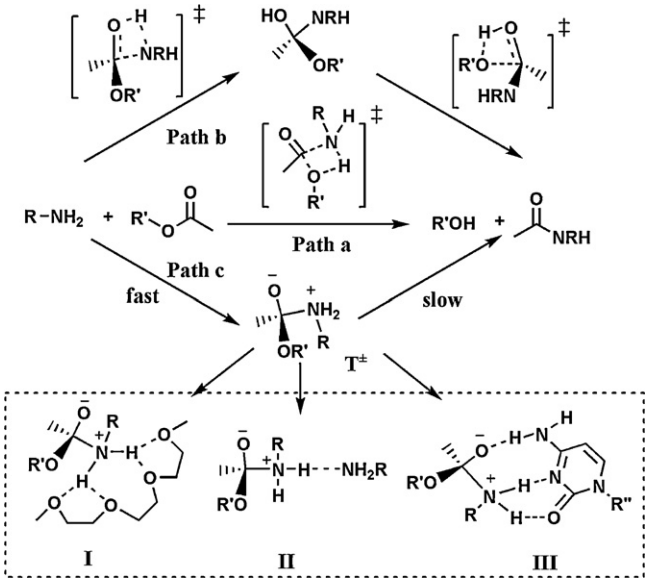


**Scheme 1.** General aminolysis reaction mechanisms.

Sung et al. [28] have studied the structures and stability of zwitterionic complexes in the aminolysis of phenyl acetate with ammonia and pointed out that at least five explicit water molecules are needed to stabilize the zwitterionic intermediate. Nevertheless, it is lack to study the whole zwitterionic pathway for the aminolysis of ester by the theoretical method.

On the other hand, the catalysts possibly stabilize the zwitterionic transition state via a hydrogen bond complex and facilitate breakdown of the zwitterionic intermediate $T^{\pm}$ to products. Many catalysts, such as polyethers [19,29–32], nucleosides [33–38], and general acid–base [13,39,40], have attracted considerable attention in experiments. As examples, possible complexes I, II, and III stabilized by catalysts are presented in Scheme 1. More recently, Fischer et al. [41] announced the reaction kinetics of *p*-nitrophenyl acetate (**1**) with *n*-butylamine (**2**) catalyzed by a series of alkyl-substituted 3-cyano-2-pyridones in deuteriochloroform. As depicted in Scheme 2, they suggested two possible concerted mechanisms I and II, but cannot rule out one of them according to experimental results. Mechanism I includes a simultaneous double-proton transfer via a favored eight-membered ring transition state (**5**), while mechanism II, like the uncatalyzed concerted process, only includes a single-proton transfer via a four-membered ring transition state (**6**). Moreover, for mechanism I, the similar process of methylamine with methyl acetate catalyzed by 2-pyridone or its tautomer 2-hydroxypridine had been explored by Zipse et al. using B3LYP/6-31G(d,p)//HF/6-31G(d,p) level of theory [18]. They deemed that the "fully concerted" pathway via the double proton-transfer transition state (mechanism I) should be the rational reaction process. They found that, starting from reactants, there were no barrier to form C—N bond in the attack of amine to acyl of ester, that is, the double-proton transfer transition state should directly link with reactants. On the contrary, Cox and Jencks suggested that the concerted double-proton transfer should have no detectable barrier and that the rate-limiting step should be the attack of amine to ester in the methoxyaminolysis of phenyl acetate catalyzed by bifunctional catalysts [42].

Some typical tautomeric bifunctional catalysts, such as 2-pyridone and oxy acids, have been exploited in the mutarotation of tetramethyl-D-glucose [43–45]. For the aminolysis reactions, such catalysis is complicated due to some different activity sites interacting with 2-pyridone or 2-hydroxypyridine, although its mode of catalysis for aminolysis [42,43,46–49] was identical with that observed in the mutarotation reaction. With our best knowledge, of theoretical studies on aminolysis reactions, few work focused on reactions promoted by bifunctional catalysts [18]. According to various kinds of mechanisms suggested for ester aminolysis catalyzed by bifunctional catalysts in experiments, in the present work, our motif is to verify a rational mechanism for title reaction, make clear the effect of 2-pyridone and 2-hydroxypyridine on the total reaction process, and remove the confusion of the rate-determining process as stated above with the density functional theory (DFT) method. Furthermore, we attempt to locate the zwitterionic transition states and would like to give a detailed picture for the whole zwitterionic mechanism. For the aminolysis reaction without catalysts, because the concerted pathway is more favorable than the stepwise pathway when esters owning a good leaving group such as *p*-nitrophenoxyl [19], we only examined the concerted mechanism to clarify the bifunctional catalysis.

## 2. Computational details

All calculations were performed using the Gaussian 03 programs [50]. The gas-phase structures were fully optimized at the B3LYP/6-31+G(d,p) level of theory [51–53]. Analytic computations of harmonic vibrational frequencies at the same level were also conducted on all critical points in order to characterize the nature of structures. All transition states were checked by intrinsic reaction coordinate (IRC) [54,55] computations to ensure each transition state linking with its two corresponding minima on the potential energy surface (PES). Natural atomic charges and Wiberg bond

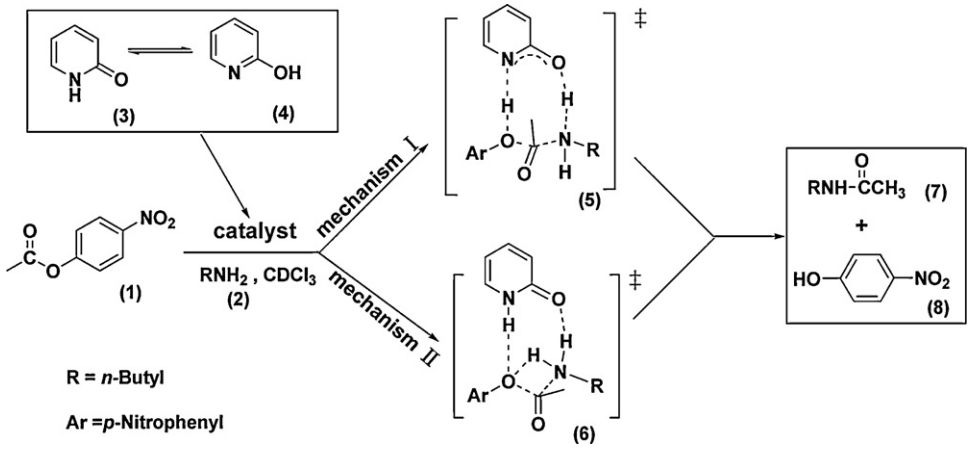


**Scheme 2.** Two assumed pathways in Ref. [41].

indices for optimized structures were also obtained using natural bond orbital (NBO) analysis [56]. In addition, in order to get more information about bond breaking/forming in some selected transition states, the percentage of bond evolution (*%Ev*), average percentage of bond evolution $(\%Ev)_{av}$ and synchronicity (*Sy*) were calculated according to expressions (1)–(3) [57].

$$(\%Ev)_i = \frac{(BO)_i^{TS} - (BO)_i^{RE}}{(BO)_i^{PR} - (BO)_i^{RE}} \times 100 \quad (1)$$

$$(\%Ev)_{av} = \frac{\sum_{i=1}^{n}(\%Ev)_i}{n} \quad (2)$$

$$Sy = 1 - \frac{\sum_{i=1}^{n}((\%Ev)_i - (\%Ev)_{av})/(\%Ev)_{av}}{2n-2} \quad (3)$$

In Eq. (1), the superscripts TS, RE, and PR refer to the transition state, reactant, and product, respectively. Practically, RE and PR refer to the two minima which link with the transition state in the reverse and forward directions, respectively. $(BO)_i$ refers to the each selected bond order in the reaction. In Eqs. (2) and (3), *n* donates the number of bonds which significantly changes from RE to PR.

Recently, Lithoxoidou and Bakalbassis [58] theoretically studied some aromatic compounds in the gas phase and solvents, and found that some solvents (dielectric constant $\varepsilon < 30$) have little effect on the gas-phase geometries (difference of bond distance < 0.004 Å, difference of angle < 1.5°). In this work, the full optimizations of the stationary points in the aminolysis mechanism without bifunctional catalysts (Path 0) were performed in chloroform ($\varepsilon = 4.9$) at the B3LYP/6-31+G(d,p) level with the CPCM model. Additionally, based on the geometries optimized in the gas phase, the single-point calculations in chloroform for the same pathway Path 0 were also carried out using the MP2/CPCM/6-31++G(d,p) method for comparison. These results are summarized in Table 1 and indicate that the small geometrical changes were induced by the presence of chloroform and the relative energies ($\Delta E$) and Gibbs free energies ($\Delta G$) by the single-point calculation were close to those obtained by the full optimization. Therefore, in view of the two points above, it is rational to conduct the single-point energy computation in chloroform based on the gas-phase optimized geometry for this work. Herein, single-point calculations at the MP2/CPCM/6-31++G(d,p) level were carried out to evaluate the solvent effect on the title reaction in chloroform [59–62]. Default parameters of chloroform implemented in the Gaussian program and the atomic radii from the UFF force field were taken in our calculations.

## 3. Results and discussions

In view of structures, both of tautomeric catalysts 2-pyridone (**3**) and 2-hydroxypyridine (**4**) can act as bifunctional catalysts. We therefore took into account three possible pathways (Scheme 3), paths A, B, and C, involving 2-pyridone or 2-hydroxypyridine as catalysts, respectively. We donated the reaction catalyzed by 2-pyridone as reaction type 1, while the reaction catalyzed by 2-hydroxypyridine as reaction type 2. Note that Scheme 3 just illustrates the diagram of reaction type 1 due to the similarity between reaction types 1 and 2. Related energies, natural charges, Wiberg Bond indices, and geometrical coordinates are presented in Supporting information.

As shown in Scheme 3, path A is a concerted process including bond formation, bond cleavage, and proton transfer. Because the bifunctional catalyst is involved into the reaction via two hydrogen bonds with substrates that is supramolecular effect, this process is similar to the concerned mechanism without catalysts. Path B includes two steps, in which the catalyst-assisted double-proton transfer from the nucleophile to the leaving group takes place followed by the return transform from the catalyst tautomer to its original conformation. Path C can be divided into three steps, nucleophilic attack on acyl, double-proton transfer via bifunctional catalyst, and elimination of the leaving group. It is very important to note that a zwitterionic intermediate is produced in the approach of amine to acyl group in the first step, whose reaction process has never been theoretically reported with an exception of the work of Lee and his coworkers [30]. In their work, the similar zwitterionic intermediate was located under the stabilization of more than five water molecules [30]. They were not concerned about the mechanism containing such intermediate, but only dealt with its stability and structure. In the following subsections, it is important to note that we will mainly describe reaction type 1 due to the similarity between reaction types 1 and 2.

### 3.1. Concerted aminolysis mechanism without bifunctional catalysts (Path 0)

Similar to our previous work [63–65], the concerted mechanism involves nucleophilic attack of *n*-butylamine to acyl of ester and simultaneous proton transfer from *n*-butylamine directly to the leaving group *p*-nitrophenoxyl. There is only one step via the four-membered ring transition state P0_TS towards the formation of $C_1$—$N_1$ bond and cleavage of $C_1$—$O_1$ bond. IRC calculations exhibit that the transition state P0_TS directly links with the pre-reactive precursor P0_RC and the product complex P0_PC in the reverse and forward directions, respectively. P0_RC is stabilized by the weak C—H···N hydrogen bond with a length of 2.436 Å, while P0_PC is stabilized by a strong hydrogen bond OH···N (2.085 Å). In PA_TS, bond distances of $C_1$—$N_1$, $N_1$—$H_1$, $H_1$—$O_1$ and $O_1$—$C_1$ are 1.600, 1.039, 1.761, and 2.094 Å, respectively, whereas their corresponding percentage of bond evolution (*%Ev*) is 64.94%, 21.42%, 8.64%, and 73.14%, indicating that proton transfer lags behind $C_1$—$N_1$ bond formation and $C_1$—$O_1$ bond cleavage. The corresponding value of synchronicity is 0.572, clearly indicating that P0_TS is a concerted but asynchronous transition state. It was proposed that P0_TS can be termed as ion-pair-like transition state [19]. Natural group charges on cationic unit (acrylamide) and anionic unit (*p*-nitrophenoxyl) are 0.814 and −0.814 au, respectively, indicating that the ion-pair character is remarkable. The four atoms $C_1$, $N_1$, $H_1$, and $O_1$ in P0_TS are almost coplanar but with a relative sharp $N_1$—$H_1$—$O_1$ bond angle

**Table 1**
Calculated equilibrium distances (Å) and relative energies (kcal/mol) for the full optimization (Opt) at the B3LYP/CPCM/6-31+G(d,p) level and single-point (Sp) calculations at the MP2/CPCM/6-31++G(d,p)//B3LYP/6-31+G(d,p) level in chloroform in the aminolysis mechanism without bifunctional catalysts for comparison.

| | | Bond length | | | | Relative energy | |
|---|---|---|---|---|---|---|---|
| | | $C_1$—$O_1$ | $C_1$—$N_1$ | $N_1$—$H_1$ | $O_1$—$H_1$ | $\Delta E$ | $\Delta G$ |
| P0_RC | Opt | 1.380 | 4.229 | 1.022 | 5.073 | 0.0 | 0.0 |
| | Sp | 1.387 | 4.504 | 1.018 | 5.126 | 0.0 | 0.0 |
| P0_TS | Opt | 1.928 | 1.593 | 1.025 | 2.071 | 13.4 | 18.0 |
| | Sp | 2.094 | 1.599 | 1.039 | 1.761 | 13.7 | 18.3 |
| P0_PC | Opt | 3.400 | 1.383 | 2.073 | 0.980 | −13.3 | −12.8 |
| | Sp | 3.418 | 1.395 | 2.085 | 0.978 | −12.3 | −11.8 |

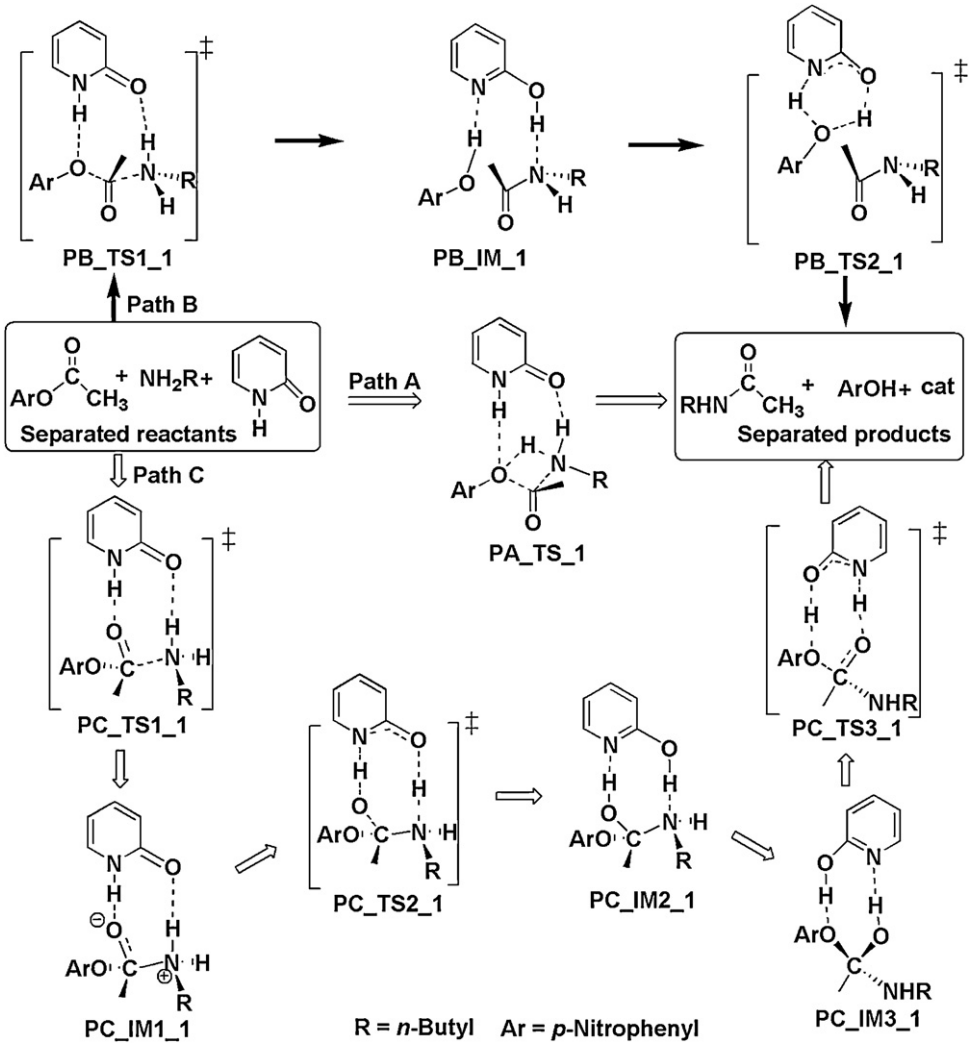


**Scheme 3.** Three possible pathways, A, B, and C, in the aminolysis reaction promoted by 2-pyridone.

(115.7°), indicating that the ring strain somewhat hinders the proton $H_1$ transferring from $N_1$ to $O_1$.

Fig. 1 indicates that the Gibbs free energy barrier is 34.0 kcal/mol from the separated reactants in the gas phase, while it decreases to 24.1 kcal/mol in chloroform. Our calculations show that the complex P0_RC is not stable in chloroform.

### 3.2. Aminolysis mechanisms with bifunctional catalysts

#### 3.2.1. Path A: concerted mechanism with the catalyst as a supramolecular effect

As stated above, path A is a concerted mechanism and bifunctional catalysts are as the supramolecular effect. For reaction type 1 with 2-pyridone catalyst, as shown in Fig. 2, the located complex PA_RC_1 indicates that two strong hydrogen bonds exist between reactants and 2-pyridone catalyst. The corresponding binding energy is 10.9 kcal/mol at the B3LYP/6-31+G(d,p) level in the gas phase. As the same to the concerted transition state P0_TS without catalysts, the transition state PA_TS_1 is also associated with the nucleophilic attack of butylamine to acyl of *p*-nitrophenyl acetate followed by a proton shift from amine to the leaving group. Bond distances of $C_1$—$N_1$, $N_1$—$H_1$, $H_1$—$O_1$ and $O_1$—$C_1$ are 1.853, 1.019, 2.545, and 1.584 Å, respectively, whereas their corresponding *%Ev* is 42.47%, 4.69%, 0.14%, and 31.02%, indicating that $N_1$—$H_1$ bond almost has no change from PA_RC_1 to PA_TS_1 and that $H_1$ proton transfer significantly lags behind $C_1$—$N_1$ bond formation and $C_1$—$O_1$ bond cleavage. Accordingly, the value of synchronicity is only 0.416. Compared with transition state P0_TS, transition state PA_TS_1 is more reactant-like since all major *%Ev* are below 50%. Based on the results of P0_TS without catalysts, it is found that 2-pyridone strongly binds with the two moieties of ion-pair-like structure via two hydrogen bonds, indicating that the ion-pair-like structure can be stabilized by the catalyst 2-pyridone and that 2-pyridone should be regarded as a bridge to balance charges of ion pair to some extent. Actually, because of much reactant-like PA_TS_1 and low *%Ev* of $C_1$—$N_1$ and $C_1$—$O_1$, PA_TS_1 should possess more character of zwitterions than that of ion pair. Natural group charges on *n*-butylamine and *p*-nitrophenoxyl acetate are 0.602 and −0.602 au, respectively. After transition state PA_TS_1, the product complex PA_PC_1 is generated. Also, two strong hydrogen bonds between 2-pyridone and products play a role in stabilizing the product complex.

The corresponding Gibbs free energy barrier from reactants to transition state PA_TS_1 is 28.0 kcal/mol in the gas phase, indicating that it dramatically decreases by 6.0 kcal/mol from the non-catalyzed reaction due to the strong hydrogen-bond effect in PA_TS_1. The Gibbs free energy barrier in chloroform decreases to 22.1 kcal/mol, which is also 2.0 kcal/mol lower than that of the non-catalyzed reaction.

For reaction type 2 with the catalyst 2-hydroxypyridine, as shown in Fig. 3, the process is very similar to that of reaction type

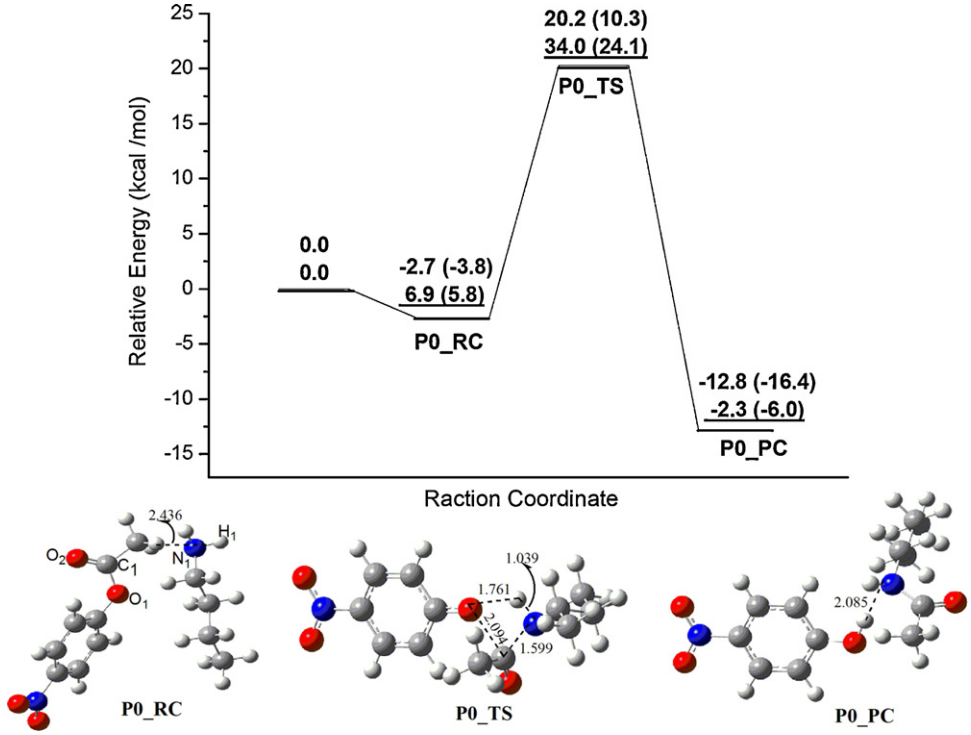


**Fig. 1.** Relative energy profile for the concerted aminolysis pathway without catalysis (in kcal/mol; top values, $\Delta E$ in the gas phase; top values in the parentheses, $\Delta E$ in chloroform; underlined values, $\Delta G$ in the gas phase; underlined values with parentheses, $\Delta G$ in chloroform. Definitions are the same in the following figures).

1. Bond distances of $C_1$—$N_1$, $C_1$—$O_1$, $H_1$—$N_1$, and $H_1$—$O_1$ in PA_TS_2 are 1.791, 1.609, 1.020, and 2.497 Å. The Gibbs free energy barrier is 30.8 and 22.7 kcal/mol in the gas phase and chloroform, respectively.

*3.2.2. Path B: stepwise mechanism including a double-proton transfer step bridged by the catalyst*

Fig. 4 indicates that, for reaction type 1 with the catalyst 2-pyridone, path B includes two steps. In the first step, we located

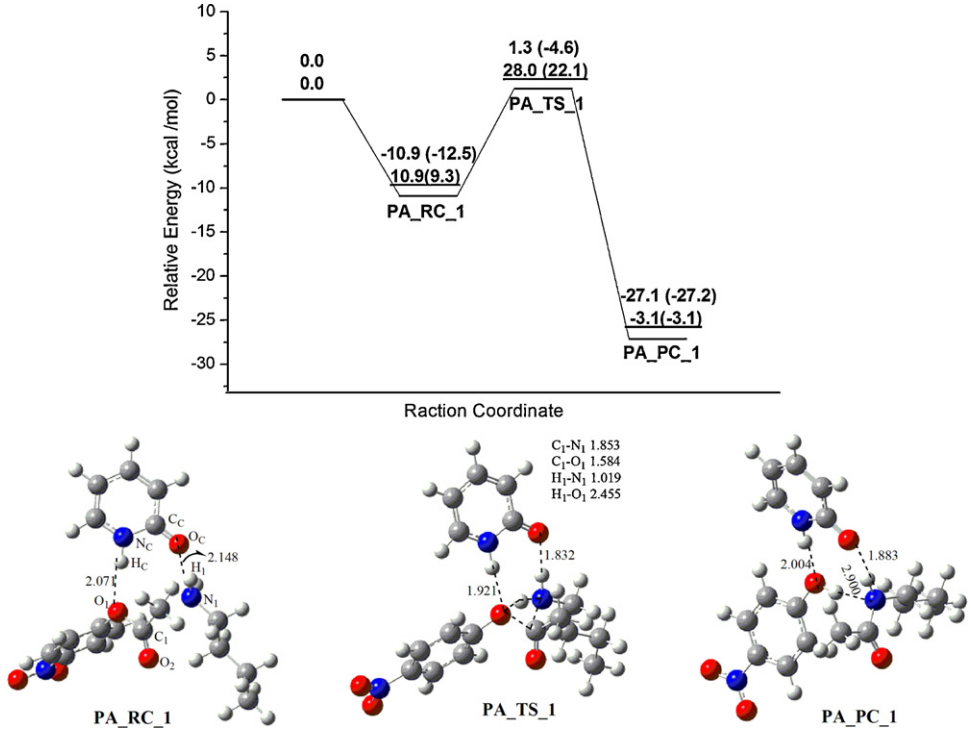


**Fig. 2.** Relative energy profile for the concerted path A of reaction type 1.

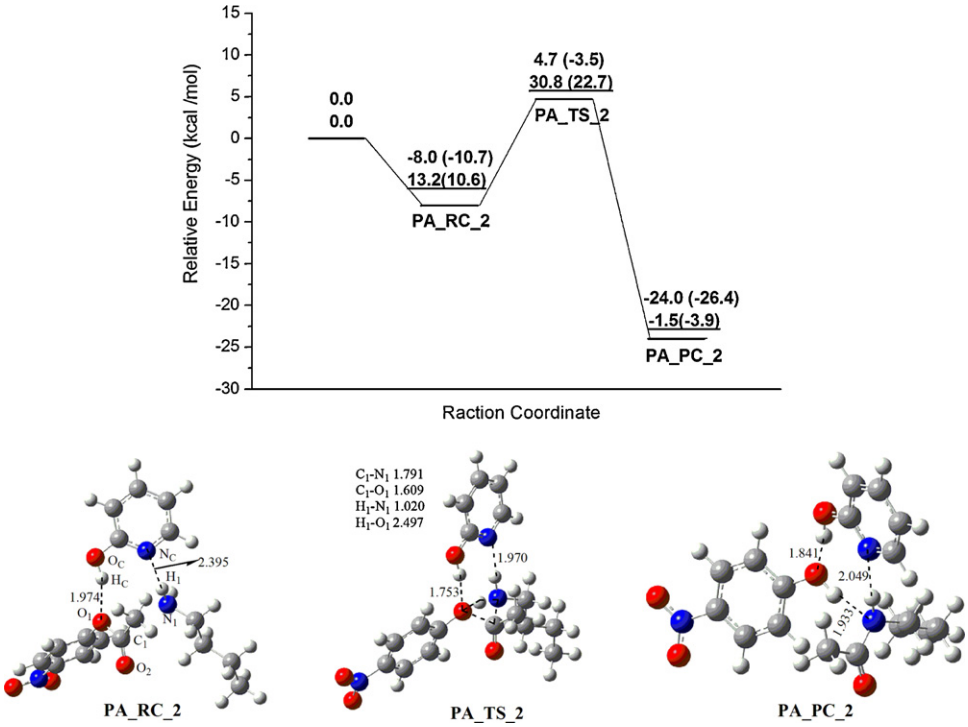


**Fig. 3.** Relative energy profile for the concerted path A of reaction type 2.

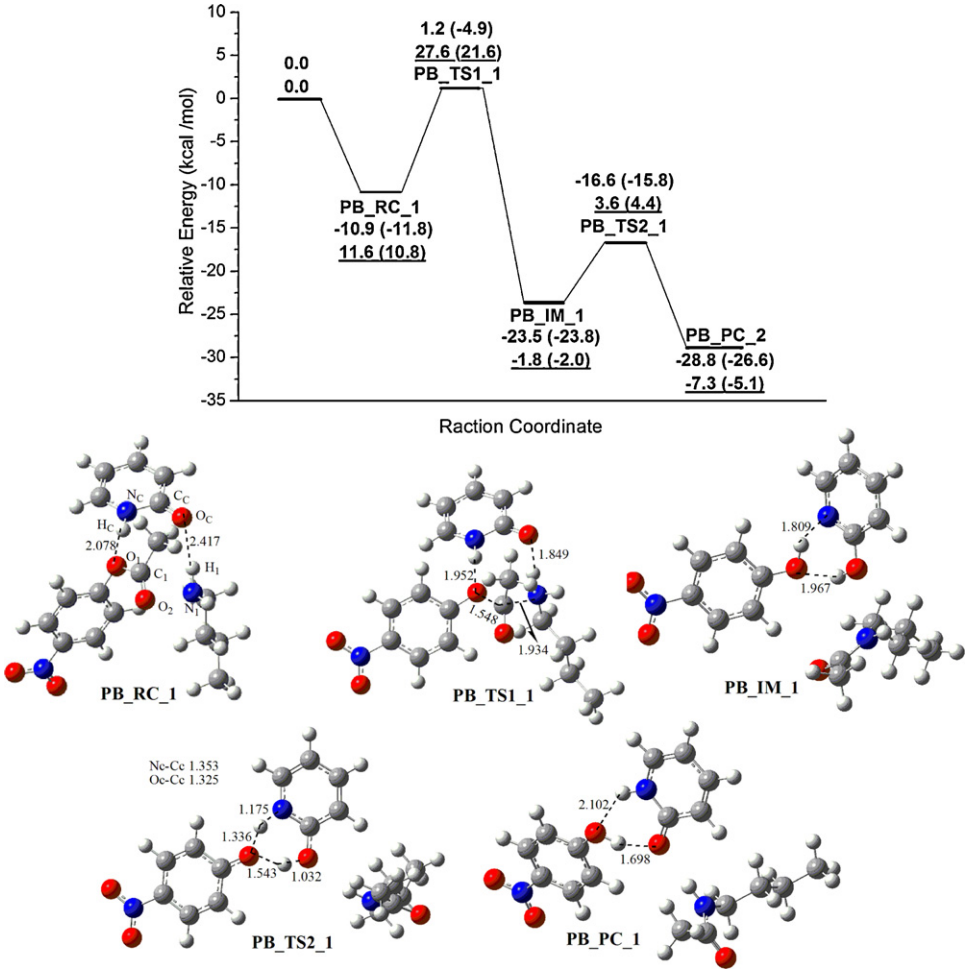


**Fig. 4.** Relative energy profile for path B of reaction type 1 including two steps.

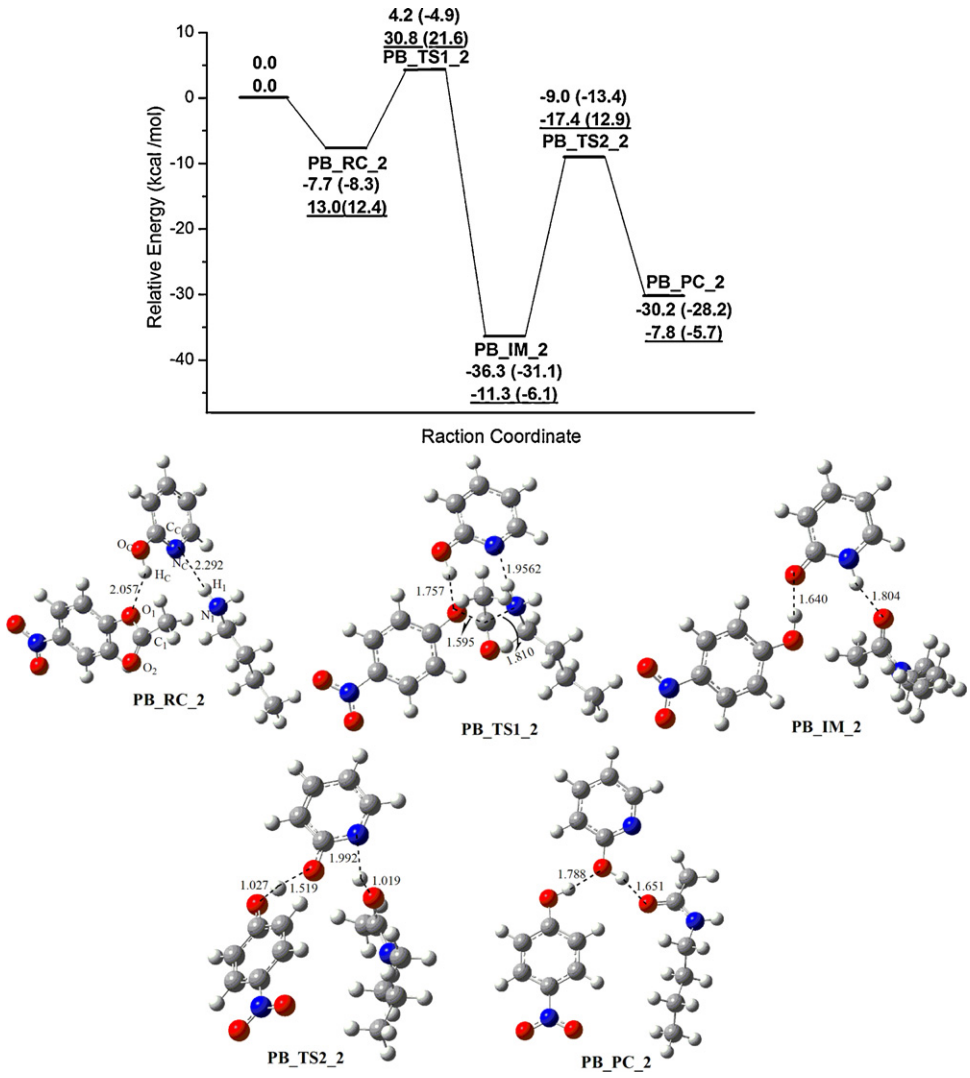


**Fig. 5.** Relative energy profile for path B of reaction type 2 including two steps.

the transition state PB_TS1_1 on the potential energy surface. Bond distances of $C_1$—$N_1$ and $C_1$—$O_1$ are 1.934 and 1.548 Å, while the corresponding *%Ev* is 35.08% and 26.46%, respectively. It is the reactant-like transition state involving the double-proton transfer bridged by the catalyst 2-pyridone. Then the intermediate PB_IM_1 is produced. Results indicate that, because $C_1$—$O_1$ bond is entirely broken and $H_1$ atom attaches at $O_c$ atom, PB_IM_1 should consist of two product molecules (amide and *p*-nitrophenol) stabilized by two very strong hydrogen bonds from the tautomeric form 2-hydroxypyridine of catalyst 2-pyridone. Distances of $O_1$—$H_c$ and $O_c$—$H_1$ bonds are 0.995 and 0.979 Å, respectively. In second step, 2-hydroxypyridine returns to the original catalyst 2-pyridone through the transfers of $H_c$ to $N_c$ atom and $H_1$ to $O_1$ atom with the help of the product *p*-nitrophenol. The corresponding transition state PB_TS2_1 was located at the B3LYP/6-31+G(d,p) level. Bond distances of $O_c$—$C_c$, $N_c$—$C_c$, $N_c$—$H_c$, $O_1$—$H_c$, $O_1$—$H_1$ and $O_c$—$H_1$ are, 1.352, 1.353, 1.175, 1.336, 1.534 and 1.032 Å, whereas the corresponding *%Ev* is 22.03, 40.72, 56.94, 59.13, 20.21 and 22.82, respectively. Meanwhile, the redistribution of the delocalized conjugated electron density of 2-pyridone should occur with the double-proton transfer, rendering the reduction of $C_c$—$O_c$ bond and the elongation of $C_c$—$N_c$ bond. From the synchronicity value of PB_TS2_1, it is clear that the process is slightly asynchronous and that the transition state PB_TS2_1 is reactant-like, namely, like PB_IM_1. After PB_TS2_1, the product complex PB_PC_1 is located.

As shown in Fig. 4, the Gibbs free energy barrier of the first step is 27.6 kcal/mol from the separated reactants in the gas phase, while it decreases to 21.6 kcal/mol in chloroform. As the same to path A, the reactant complex also cannot be stable in chloroform. For the second step, we found that the Gibbs free energy barriers from PB_IM_1 to PB_TS2_1 are 5.4 and 6.4 kcal/mol in the gas phase and in chloroform, respectively. That is to say, in the complete process of path B, it turns out that the rate-determining step is to overcome the transition state PB_TS_1.

Also for reaction type 2 in path B, as shown in Fig. 5, it is also very similar to that of reaction type 1 as stated above. The rate-determining step is to overcome the transition state PB_TS1_2. Bond distances of $C_1$—$N_1$ and $C_1$—$O_1$ are 1.810 and1.595 Å, respectively. Then it is followed by a return of the tautomeric form 2-pyridone of catalyst to the original 2-hydroxypyridine. The Gibbs free energy barrier in the rate-determining step is 30.8 kcal/mol in the gas phase and 21.6 kcal/mol in chloroform, respectively.

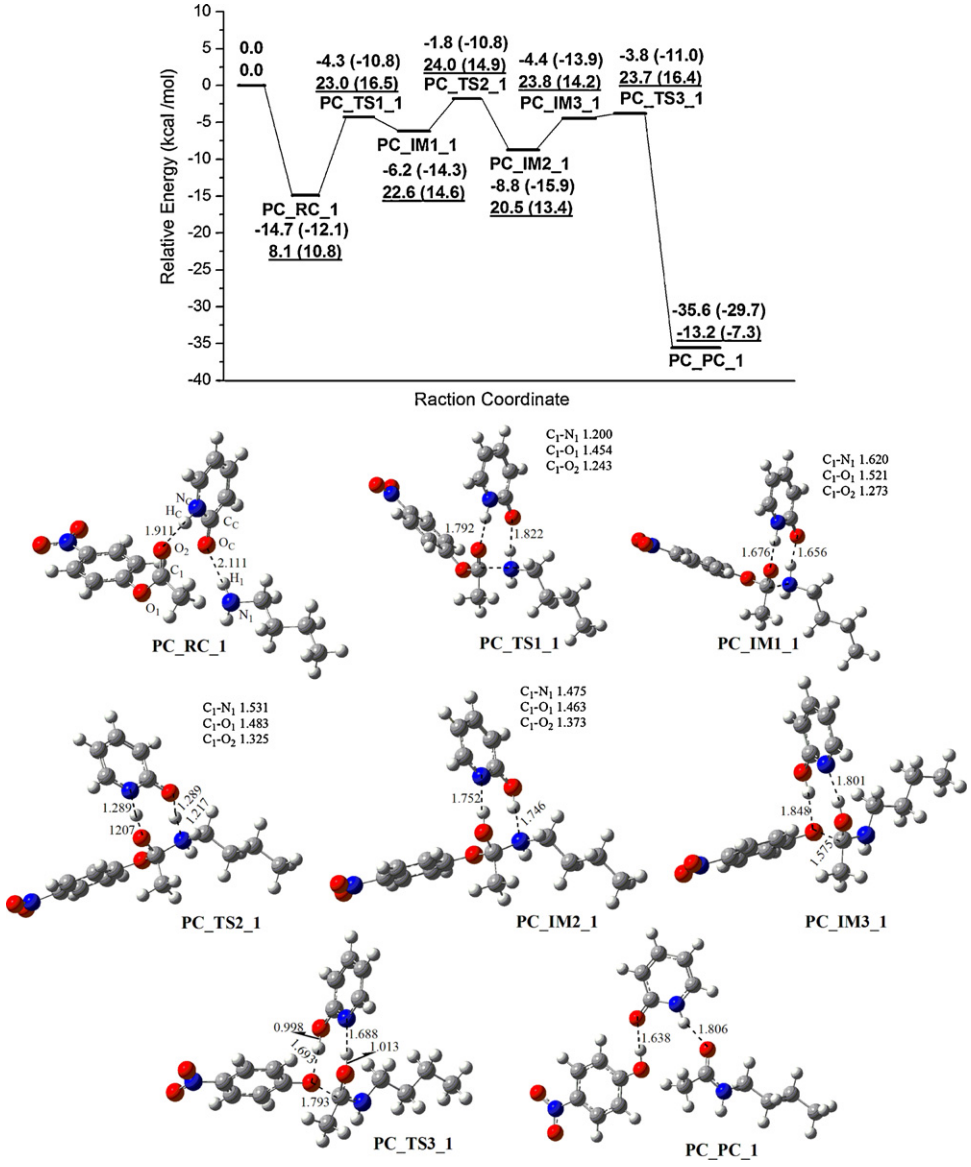


**Fig. 6.** Relative energy profile for path C of reaction type 1 including three steps.

### 3.2.3. Path C: stepwise mechanism including a zwitterionic tetrahedral intermediates

For aminolysis reactions without any catalysts, there are two possible pathways based on theoretical results. One is concerted as stated above, and the other is neutral stepwise including a neutral tetrahedral intermediate. In the neutral stepwise mechanism, it mainly includes two steps: nucleophilic addition on acyl and elimination of leaving group. Here, we investigated the title reaction via path C as following, where the catalyst 2-pyridone binds with $H_1$ and $O_2$ atoms (Fig. 6). Different from the uncatalyzed stepwise mechanism, path C mainly includes three steps. Interestingly, a zwitterionic intermediate is found in path C.

In the first step, as shown in Fig. 6, the transition state PC_TS1_1 betrays that this step is a nucleophilic attack of *n*-butylamine to acyl of *p*-nitrophenyl acetate. Bond distance of $N_1$—$C_1$ is 1.920 Å. Analysis of frequencies exhibits that the imaginary frequency ($151.79i\,cm^{-1}$) is almost purely associated with the $N_1$—$C_1$ bond stretching mode. Then the intermediate PC_IM1_1 is produced. The $N_1$—$C_1$ bond distance is 1.620 Å, which is only 0.30 Å shorter than that of PC_TS1_1. Interestingly, it is found that the elongation of $C_1$—$O_1$ bond of leaving group rather than $C_1$=$O_2$ double bond, namely, electrons transfer to $\sigma^*_{C_1-O_1}$ instead of $\pi^*_{C_1=O_2}$ orbital, takes place with the approach of *n*-butylamine, which should also be resulted from the effect of the good leaving group. The $C_1$—$O_1$ bond length changes from 1.368 Å in PC_RC_1 to 1.521 Å in PC_IM1_1, whereas $C_1$=$O_2$ bond length elongates by only 0.057 Å. Wiberg bond order calculations show that %*Ev* of $N_1$—$C_1$ is 61.52%. It turns out that the intermediate PC_IM1_1 resembles the transition state PC_TS1_1 and that PC_TS1_1 is a product-like late transition state. Generally, for PC_IM1_1, it should be regarded as a zwitterionic structure. The zwitterionic character of PC_IM1_1 can be seen from the negative charge of $O_2$ increasing by −0.177 au and the negative charge of $N_1$ decreasing by −0.235 au relative to reaction complex.

In the second step, we located the transition state PC_TS2_1, which corresponds to the double-proton transfer from $N_1$ to $O_2$ with the assistance of 2-pyridone. Bond distances of $O_2$—$H_c$, $N_c$—$H_c$, $O_c$—$H_1$, and $N_1$—$H_1$ are 1.207, 1.289, 1.289, and 1.217 Å, whereas the corresponding %*Ev* is 51.89%, 48.07%, 41.63%, and 40.48%, indicating that $H_1$ transfer lags behind $H_c$ transfer. From the intermediate PC_IM2_1 generated via PC_TS2_1, we found that it is a tetrahedral intermediate, that is, $N_1$ atom completely binds with $C_1$ atom and $C_1$—$O_2$ is a single bond with $H_c$ attaching at $O_2$ atom. It is

important to note that the elongated $C_1$—$O_1$ bond in PC_IM1_1 restores to 1.463 Å in PC_IM2_1 due to the formation of $C_1$—$O_2$ single bond. Furthermore, the catalyst 2-pyridone changes to 2-hydroxypyridine after the double-proton transfer in this step.

In the third step, we planned to determine a process to eliminate the leaving group. Unfortunately all attempts to locate an intermediate from the initial-guess structure, in which one of hydrogen bond is related with $O_1$ atom instead of $N_1$ atom in PC_IM2_1 without $N_1$ inversed, are failed. It is rational to lead to this result because the negative charge of $N_1$ is more than that of $O_1$ and there is no hindrance for 2-hydroxypyridine to rotate from $O_1$ to $N_1$. However, according to our previous similar results [65], it should be free to undergo the inversion of amine group. In this way, the hydrogen bond heading to the lone pair of $N_1$ atom is blocked after the inversion of amine and it has to form with $O_1$ atom. The corresponding structure PC_IM3_1 indicates that $C_1$—$O_1$ bond elongates again (1.575 Å) due to the formed strong hydrogen bond $O_1$—$H_c$. From our calculations, it is easy to locate the transition state PC_TS3_1 connection PC_IM3_1 and products. Unexpectedly, the imaginary frequency shows that the vibrational mode is mainly associated with the $C_1$—$O_1$ bond stretch instead of the double-proton transfer. The distance of $C_1$—$O_1$ is 1.793 Å, which is only 0.219 Å longer than that in PC_IM3_1. *%Ev* of $C_1$—$O_1$ is 31.22% and the double protons almost have no change, implying that PC_TS3_1 is a reactant-like early transition state. At last, the product complex PC_PC_1 is produced and it is found that the double protons have already transferred with the assistance of 2-hydroxypyridine and that the catalyst restores to 2-pyridone.

From the complete path C as stated above, it is found that the difference of the catalyst effect occurs in each step. In the first step, the catalyst 2-pyridone should be regarded as the supramolecular effect, while in the second and third step, the catalyst 2-pyridone or 2-hydroxypyridine assist in the aminolysis reaction as a bridge of proton transfer.

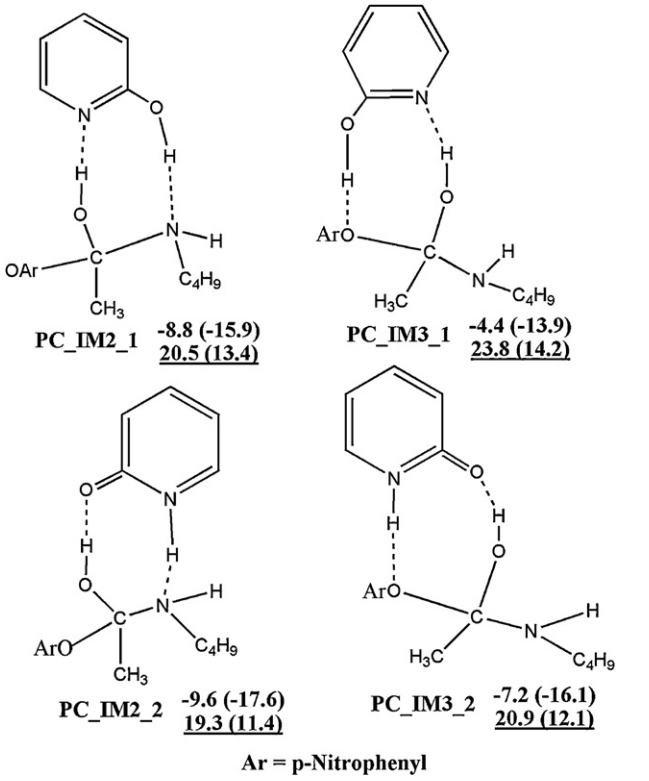


**Fig. 7.** Four possible intermediates and their relative energies in path C of reaction types 1 and 2.

**Table 2**
Rate-determining Gibbs free energy barriers (kcal/mol) for three possible pathways with bifunctional catalysts in the gas phase ($\Delta G_g^{\neq}$) and in chloroform ($\Delta G_s^{\neq}$) (in kcal/mol).

| | Type 1 | | Type 2 | |
|---|---|---|---|---|
| | $\Delta G_g^{\neq}$ | $\Delta G_s^{\neq}$ | $\Delta G_g^{\neq}$ | $\Delta G_s^{\neq}$ |
| Path A | 28.0 | 22.1 | 30.8 | 22.7 |
| Path B | 27.6 | 21.6 | 30.8 | 21.6 |
| Path C | 24.0 | 16.5 | 27.2 | 18.0 |

As shown in Fig. 6, the energy diagram indicates that the rate-determining step may be the formation of the intermediate PC_IM3_1 in the gas phase. However, as discussed below, it should not be a correct reaction picture. Because, actually, there should be four possible structures including tetrahedral intermediates and catalysts 2-pyridone or 2-hydroxypyridine via hydrogen bonds (Fig. 7), the displacement or detachment of catalysts among the four intermediates should take place in the reaction. In addition, we found that the transition states PC_TS1_1 and PC_TS2_1 have the same relative free energies in the gas phase (−10.8 *vs.* −10.8 kcal/mol), while, in chloroform, to overcome PC_TS2_1 is changed to be slightly easier than PC_TS1_1 (14.9 *vs.* 16.5 kcal/mol). Note that the gas-phase Gibbs free energy barrier from PC_IM3_1 to PC_TS3_1 is 2.9 kcal/mol, while it decreases to 2.2 kcal/mol in chloroform. So, the rate-limiting step is the first one in chloroform.

For reaction type 2, as shown in Fig. 8, the reaction process of path C is also very similar to reaction type 1. Step 2 via the transition state PC_TS2_2 and step 1 via the transition state PC_TS1_2 may be the rate-determining steps in the gas phase and chloroform, respectively. The corresponding Gibbs free energy barrier is 27.2 and 18.0 kcal/mol in the gas phase and chloroform, respectively. Same as reaction type 1, the two intermediates, PC_IM2_2 and PC_IM3_2, are lower than separated reactants in reaction type 2. As presented in Fig. 7, PC_IM2_2 is the most stable tetrahedral intermediate in reaction types 1 and 2. Alternatively, for reaction type 1, after the formation of PC_IM2_1 via the transition state PC_TS2_1, the displacement of catalyst may occur towards the formation of PC_IM2_2, rendering that step 2 in the gas phase and step 1 in chloroform should be the rate-determining step, respectively.

Finally, in order to picture the complete title reaction and determine which pathway is more rational, Gibbs free energy barriers of the rate-determining step for each pathway in the gas phase and chloroform are presented in Table 2. We found that path C is the most favored pathway both in the gas phase and in chloroform. Compared with the uncatalyzed aminolysis, the bifunctional catalysts play an important role in title reaction and dramatically decrease the active energy barrier. Bifunctional catalysts can enhance the nucleophilicity of amine and stabilize the leaving group. Moreover, the bifunctional catalysts, as proton shuttles, can help protons linearly transfer to dramatically decrease the energy barrier. According to the reported results that the energy difference between 2-pyridone and 2-hydroxypyridine is about 1.0 kcal/mol [66], it seems safe to say that both 2-pyridone and 2-hydroxypyridine can exist in real reaction system, rendering that, because of the close reaction activation energy, it is possible for aminolysis to follow path C using 2-pyridone or 2-hydroxypyridine as the catalyst. In this work, our results reveal a new possible mechanism and renovate the aminolysis reaction promoted by bifunctional catalysts. Most of all, we put forward that it is crucial to generate the zwitterionic intermediate in aminolysis reaction.

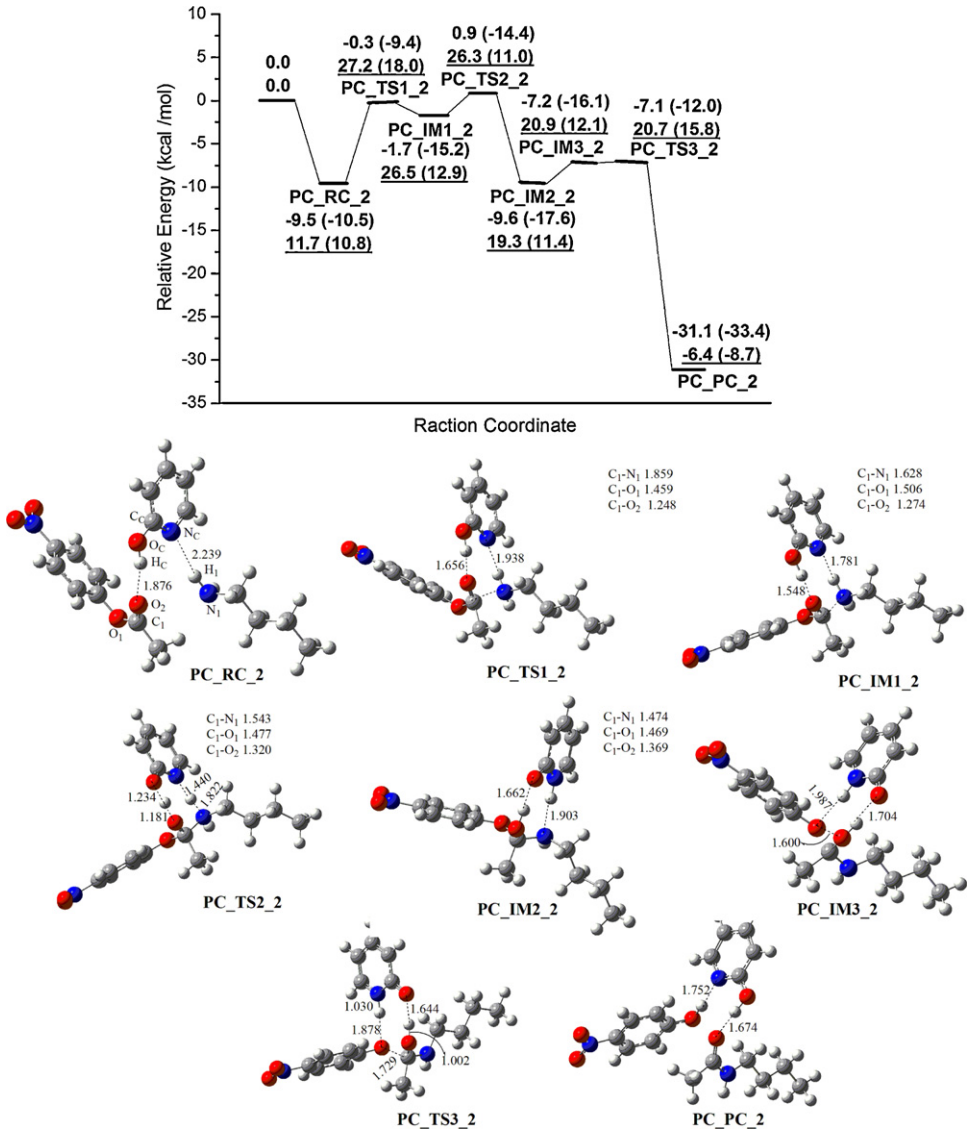


**Fig. 8.** Relative energy profile for path C of reaction type 2 including three steps.

## 4. Conclusion

In the present theoretical study of aminolysis of *p*-nitrophenyl acetate with *n*-butylamine catalyzed by 2-pyridone and its tautomeric form 2-hydroxypyridine, we have examined three possible mechanisms. Path A is concerted via a four-membered ring transition state including the supramolecular effect of the catalyst. Path B includes two sequential steps, where the double-proton transfer via an eight-membered ring transition state bridged by the catalyst is the rate-determining process followed by the restore of the catalyst conformation. Path C is zwitterionic stepwise, which has never been theoretically found in aminolysis of ester without any catalyst. Our calculations indicate that the third mechanism is the most favored pathway. The Gibbs free energy barrier for the rate-determining step of path C is 24.0 and 16.5 kcal/mol in the gas phase and chloroform for reaction type 1, while 27.2 and 18.0 kcal/mol in the gas phase and chloroform for reaction type 2, respectively. Anyway, the mechanism catalyzed by 2-pyridone or 2-hydroxypyridine is more favorable than the uncatalyzed reaction. Our results indicate that bifunctional catalysts can accelerate the title reaction not only with supramolecular effect but also as proton shuttles. This finding should be helpful for the insight on the function of nucleosides in the aminolysis of ester.

## Acknowledgments

This project has been supported by the National Natural Science Foundation of China (Grant Nos. 21173151 and 20835003) and National Basic Research Program of China (973 Program) (Grant No. 2011CB201202).

## Appendix A. Supplementary data

Supplementary data associated with this article can be found, in the online version, at doi:10.1016/j.molcata.2011.12.003.

## References

[1] J.F. Bunnett, G.T. Davis, J. Am. Chem. Soc. 82 (1960) 665–674.
[2] W.P. Jencks, J. Carriuolo, J. Am. Chem. Soc. 82 (1960) 675–681.
[3] T.C. Bruice, M.F. Mayahi, J. Am. Chem. Soc. 82 (1960) 3067–3071.
[4] T.C. Bruice, R.G. Willis, J. Am. Chem. Soc. 87 (1965) 531–536.
[5] W.P. Jencks, M. Gilchrist, J. Am. Chem. Soc. 88 (1966) 104–108.

[6] L.R. Fedor, T.C. Bruice, K.L. Kirk, J. Meinwald, J. Am. Chem. Soc. 88 (1966) 108–111.
[7] T.C. Bruice, A. Donzel, R.W. Huffman, A.R. Butler, J. Am. Chem. Soc. 89 (1967) 2106–2121.
[8] G.M. Blackburn, W.P. Jencks, J. Am. Chem. Soc. 90 (1968) 2638–2645.
[9] W.P. Jencks, M. Gilchrist, J. Am. Chem. Soc. 90 (1968) 2622–2637.
[10] T.C. Bruice, S.M. Felton, J. Am. Chem. Soc. 91 (1969) 2799–2800.
[11] T.C. Bruice, A.F. Hegarty, S.M. Felton, A. Donzel, N.G. Kundu, J. Am. Chem. Soc. 92 (1970) 1370–1378.
[12] F.M. Menger, J.H. Smith, Tetrahedron Lett. 48 (1970) 4163–4168.
[13] F.M. Menger, J.H. Smith, J. Am. Chem. Soc. 94 (1972) 3824–3829.
[14] C.C. Yang, W.P. Jencks, J. Am. Chem. Soc. 110 (1988) 2972–2973.
[15] T. Oie, G.H. Loew, S.K. Burt, J.S. Binkley, R.D. MacElroy, J. Am. Chem. Soc. 104 (1982) 6169–6174.
[16] T. Oie, G.H. Loew, S.K. Burt, R.D. MacElroy, J. Am. Chem. Soc. 105 (1983) 2221–2227.
[17] J.H. Jensen, K.K. Baldridge, M.S. Gordon, J. Phys. Chem. 96 (1992) 8340–8351.
[18] L.-H. Wang, H. Zipse, Liebigs Ann. (1996) 1501–1509.
[19] H. Zipse, L-.h. Wang, K.N. Houk, Liebigs Ann. (1996) 1511–1522.
[20] H. Adalsteinsson, T.C. Bruice, J. Am. Chem. Soc. 120 (1998) 3440–3447.
[21] S. Chalmet, W. Harb, M.F. Ruiz-Lopez, J. Phys. Chem. A 105 (2001) 11574–11581.
[22] W. Yang, D.G. Drueckhammer, Org. Lett. 2 (2000) 4133–4136.
[23] S. Ilieva, B. Galabov, D.G. Musaev, K. Morokuma, H.F. Schaefer III, J. Org. Chem. 68 (2003) 1496–1502.
[24] S. Ilieva, B. Galabov, D.G. Musaev, K. Morokuma, J. Org. Chem. 68 (2003) 3406–3412.
[25] B. Galabov, Y. Atanasov, S. Ilieva, H.F. Schaefer III, J. Phys. Chem. A 109 (2005) 11470–11474.
[26] L. Jin, Y. Wu, Y. Xue, Y. Guo, D.Q. Xie, G.S. Yan, Acta Chim. Sin. 64 (2006) 873–878.
[27] D.A. Singleton, S.R. Merrigan, J. Am. Chem. Soc. 122 (2000) 11035–11036.
[28] D.D. Sung, I.S. Koo, K. Yang, I. Lee, Chem. Phys. Lett. 426 (2006) 280–284.
[29] R.D. Gandour, D.A. Walker, A. Nayak, G.R. Newkome, J. Am. Chem. Soc. 100 (1978) 3608–3609.
[30] J.C. Hogan, R.D. Gandour, J. Am. Chem. Soc. 102 (1980) 2865–2866.
[31] J.C. Hogan, R.D. Gandour, J. Org. Chem. 56 (1991) 2821–2826.
[32] J.C. Hogan, R.D. Gandour, J. Org. Chem. 57 (1992) 55–61.
[33] R.J. Pieters, I. Huc, J. Rebek Jr., Chem. Eur. J. 1 (1995) 183–192.
[34] I. Huc, R.J. Pieters, J. Rebek Jr., J. Am. Chem. Soc. 116 (1994) 11592–19593.
[35] C. Melander, D.A. Horne, J. Org. Chem. 61 (1996) 8344–8346.
[36] C. Melander, D.A. Horne, J. Org. Chem. 62 (1997) 9295–9297.
[37] M. Tominaga, K. Konishi, T. Aida, J. Am. Chem. Soc. 121 (1999) 7704–7705.
[38] D. Suarez, K.M. Merz Jr., J. Am. Chem. Soc. 123 (2001) 7687–7690.
[39] F.M. Menger, A.C. Vitale, J. Am. Chem. Soc. 95 (1973) 4931–4934.
[40] C. Su, J.W. Watson, J. Am. Chem. Soc. 96 (1974) 1847–1854.
[41] C.B. Fischer, H. Steininger, D.S. Stephenson, H. Zipse, J. Phys. Org. Chem. 18 (2005) 901–907.
[42] M.M. Cox, W.P. Jencks, J. Am. Chem. Soc. 103 (1981) 580–587.
[43] P.R. Rony, J. Am. Chem. Soc. 91 (1969) 6090–6096.
[44] P.R. Rony, J. Am. Chem. Soc. 90 (1968) 2824–2831.
[45] P.R. Rony, R.O. Neff, J. Am. Chem. Soc. 95 (1973) 2896–2905.
[46] C.G. Swain, J.F. Brown Jr., J. Am. Chem. Soc. 74 (1952) 2538–2543.
[47] F.M. Menger, J. Am. Chem. Soc. 88 (1966) 3081–3084.
[48] H. Anderson, C. Su, J.W. Watson, J. Am. Chem. Soc. 91 (1969) 482–484.
[49] J.C. Fishbein, H. Baum, M.M. Cox, W.P. Jencks, J. Am. Chem. Soc. 109 (1987) 5790–5800.
[50] M.J. Frisch, G.W. Trucks, H.B. Schlegel, G.E. Scuseria, M.A. Robb, J.R. Cheeseman, V.G. Zakrzewski, J.A. Montgomery, R.E. Stratmann, J.C. Burant, S. Dapprich, J.M. Millam, A.D. Daniels, K.N. Kudin, M.C. Strain, O. Farkas, J. Tomasi, V. Barone, M. Cossi, R. Cammi, B. Mennucci, C. Pomelli, C. Adamo, S. Clifford, J. Ochterski, G.A. Petterson, P.Y. Ayala, Q. Cui, K. Morokuma, D.K. Malick, A.D. Rabuck, K. Raghavachari, J.B. Foresman, J. Cioslowski, J.V. Ortiz, B.B. Stefanov, G. Liu, A. Liashenko, P. Piskorz, I. Komaromi, R. Gomperts, R.L. Martin, D.J. Fox, T. Keith, M.A. Al-Laham, C.Y. Peng, A. Nanayakkara, C. Gonzalez, M. Challacombe, P.M.W. Gill, B.G. Johnson, W. Chen, M.W. Wong, J.L. Andres, M. Head-Gordon, E.S. Replogle, J.A. Pople, Gaussian 03 (Revision D.01), Gaussian, Inc., Wallingford, CT, 2005.
[51] B. Miehlich, A. Savin, H. Stoll, H. Preuss, Chem. Phys. Lett. 157 (1989) 200–206.
[52] C. Lee, W. Yang, R.G. Parr, Phys. Rev. B 37 (1998) 785–789.
[53] A.D. Becke, J. Chem. Phys. 98 (1993) 5648–5652.
[54] C. Gonzalez, H.B. Schlegel, J. Chem. Phys. 90 (1989) 2154–2161.
[55] C. Gonzalez, H.B. Schlegel, J. Phys. Chem. 94 (1990) 5523–5527.
[56] E. Reed, L.A. Curtiss, F. Weinhold, Chem. Rev. 88 (1988) 899–926.
[57] A. Moyano, M. Pericàs, A. Valentí, J. Org. Chem. 54 (1989) 382–573.
[58] A.T. Lithoxoidou, E.G. Bakalbassis, J. Phys. Chem. A 109 (2005) 366–377.
[59] M.T. Cances, B. Mennucci, J. Tomasi, J. Chem. Phys. 107 (1997) 3020–3041.
[60] B. Mennucci, J. Tomasi, J. Chem. Phys. 106 (1997) 5151–5158.
[61] B. Mennucci, E. Cances, J. Tomasi, J. Phys. Chem. B 101 (1997) 10506–10517.
[62] J. Tomasi, B. Mennucci, E. Cances, J. Mol. Struct. 464 (1999) 211–226.
[63] L. Jin, Y. Xue, H. Zhang, C.K. Kim, D.Q. Xie, G.S. Yan, J. Phys. Chem. A 112 (2008) 4501–4510.
[64] G.Q. Yi, Y. Zeng, X.F. Xia, Y. Xue, C.K. Kim, G.S. Yan, Chem. Phys. 345 (2008) 73–81.
[65] Y. Wu, L. Jin, Y. Xue, D.Q. Xie, C.K. Kim, Y. Guo, G.S. Yan, J. Comput. Chem. 29 (2008) 1222–1232.
[66] M.K. Hazra, T. Chakraborty, J. Phys. Chem. A 110 (2006) 9130–9136.